

## dc properties of series-parallel arrays of Josephson junctions in an external magnetic field

S. J. Lewandowski

*Instytut Fizyki, Polska Akademia Nauk, Al. Lotnikow 32, PL 02-668 Warszawa, Poland*

(Received 1 June 1990; revised manuscript received 12 February 1991)

A detailed dc theory of superconducting multijunction interferometers has previously been developed by several authors for the case of parallel junction arrays. The theory is now extended to cover the case of a loop containing several junctions connected in series. The problem is closely associated with high- $T_c$  superconductors and their clusters of intrinsic Josephson junctions. These materials exhibit spontaneous interferometric effects, and there is no reason to assume that the intrinsic junctions form only parallel arrays. A simple formalism of phase states is developed in order to express the superconducting phase differences across the junctions forming a series array as functions of the phase difference across the weakest junction of the system, and to relate the differences in critical currents of the junctions to gaps in the allowed ranges of their phase functions. This formalism is used to investigate the energy states of the array, which in the case of different junctions are split and separated by energy barriers of height depending on the phase gaps. Modifications of the washboard model of a single junction are shown. Next a superconducting inductive loop containing a series array of two junctions is considered, and this model is used to demonstrate the transitions between phase states and the associated instabilities. Finally, the critical current of a parallel connection of two series arrays is analyzed and shown to be a multivalued function of the externally applied magnetic flux. The instabilities caused by the presence of intrinsic serial junctions in granular high- $T_c$  materials are pointed out as a potential source of additional noise.

### I. INTRODUCTION

The existence of intrinsic Josephson junctions in granular high- $T_c$  superconductors is a well-established fact. The evidence includes a variety of interferometric effects in externally applied magnetic field, e.g., operation of rf SQUID's made from single-connected bulk samples<sup>1</sup> or magnetically tuned microwave noise emission from thin films.<sup>2</sup> These effects clearly indicate that at least some of the intrinsic junctions are connected into closed loops and, in the case of dc current bias applied to the sample, such loops may be distributed along the percolation path.

If one tries to imagine the arrangement of junctions in a loop, it appears to be rather obvious that some of them may be series connected and others parallel connected. In fact, in some of the experiments,<sup>2</sup> multiple periods in the applied field were detected, indicating multiple parallel loops of differing areas. Other studies, including the majority of high- $T_c$  SQUID measurements,<sup>3</sup> indicated a single-flux-quantum period, but were troubled by extraneous modulations, and that picture is consistent with a series configuration.

The dc behavior of parallel arrays of junctions is well understood. A detailed theory for this case was developed in the past and confirmed by ample experimental evidence.<sup>4</sup> Single-connected series arrays have also received some attention but only from the point of view of their ac properties<sup>5</sup> and in applications like parametric amplifiers or voltage standards. It was in this context, however, that the possible appearance of series arrays in high- $T_c$  superconductors was discussed.<sup>6</sup> Surprisingly enough, no work was done on the dc properties of super-

conducting loops containing what might be called series-parallel junction arrays, created by the replacement of single junctions in a parallel array by series arrays of such junctions.

In Sec. II the elementary but instructive case of a single-connected series array composed of only two junctions is considered. Stationary properties of this array are examined in terms of phase relations between component junctions, with particular attention paid to the energy-phase relations. The formalism developed for this case is, in Sec. III, applied to a loop containing two series inductances and two series arrays of junctions and is used to examine the critical current of the loop. The analytical results are discussed next in conjunction with some numerical examples. Conclusions are presented in Sec. IV.

### II. SERIES ARRAYS OF JUNCTIONS

#### A. Phase relations

We consider first a series array of (ideal) Josephson junctions in its elementary form of two junctions supplied in series from a common dc current source  $J$ . Generalization to the case of an array of  $N$  series junctions is straightforward, as will be seen in Sec. III.

Let  $I_1, \varphi_1$  be the critical current and superconducting phase difference, respectively, of the first junction and let  $I_2, \varphi_2$  be the same quantities for the second junction. Then the stationary properties of the system under consideration are described adequately by the set of Josephson equations:

$$J = I_1 \sin \varphi_1, \quad (1)$$

$$J = I_2 \sin \varphi_2, \quad (2')$$

where  $J$ ,  $\varphi_1$ ,  $\varphi_2$  are considered to be independent variables and  $I_1$ ,  $I_2$ , are parameters.

Equations (1) and (2') are subject to the obvious restraint that the absolute value of  $J$  must not exceed any of the critical currents  $I_1$ ,  $I_2$ . Assuming  $I_1 \leq I_2$ , we choose to express this restraint by replacing Eq. (2') with

$$\sin \varphi_2 = a \sin \varphi_1, \quad a = I_1 / I_2 \leq 1, \quad (2'')$$

which means that  $\varphi_2$  is no longer an independent variable but a function of  $\varphi_1$ . For this reason we will sometimes refer to  $\varphi_1$  as the driving phase, and to  $\varphi_2$  as the driven phase.

The functional dependence of the driven phase on  $\varphi_1$  can be explicitly written as

$$\varphi_2(\varphi_1) = \arcsin(a \sin \varphi_1). \quad (2''')$$

However, arcsin is not a unique function of its argument and that might be shown explicitly as well. Designating  $\varphi_2^{(0)}$  by the principal branch of arcsin in Eq. (2'''),

$$\varphi_2^{(0)} = \arcsin(a \sin \varphi_1), \quad \varphi_2^{(0)} \in \mathcal{R}'_0,$$

where

$$\mathcal{R}'_0 = [-\pi/2, \pi/2],$$

we arrive at the final version of Eq. (2');

$$\varphi_2(\varphi_1) = \varphi_2^{(m)} = (-1)^m \varphi_2^{(0)} + m\pi, \quad (2)$$

where  $m$  is an integer.

Some reflection will show that the range  $\mathcal{R}_0$  of  $\varphi_2^{(0)}$  can be narrowed down to

$$\mathcal{R}_0 = [-(\pi/2 - \Psi), \pi/2 - \Psi],$$

where

$$\Psi = \arccos a, \quad \Psi \in [0, \pi/2]. \quad (2a)$$

More generally, the range  $\mathcal{R}_m$  of  $\varphi_2^{(m)}$  is

$$\mathcal{R}_m = [(2m - 1)\pi/2 + \Psi, (2m + 1)\pi/2 - \Psi]. \quad (2b)$$

It is seen that each range  $\mathcal{R}_m$  is centered around  $m\pi$ , has a length of  $\pi - 2\Psi$ , and is separated from its neighbors by gaps (range of forbidden  $\varphi_2$  values) of length  $2\Psi$ , centered around odd multiples of  $\pi/2$ . For  $a = 0$ , i.e., infinite critical current  $I_2$ , the range  $\mathcal{R}_m$  shrinks to a single point  $m\pi$ . Conversely, for  $a = 1$ , i.e.,  $I_2 = I_1$ , the range  $\mathcal{R}_m$  shares its limits with its neighbors and the gaps become void.

Observe that, from Eq. (2), we have

$$\varphi_2^{(m)} + 2\pi = \varphi_2^{(m+2)} \quad (3a)$$

and

$$\varphi_2^{(m)} + \varphi_2^{(m+1)} = (2m + 1)\pi. \quad (3b)$$

The above two relations provide convenient means for changing the representation of  $\varphi_2$ . Only one even repre-

sentation, say  $\varphi_2^{(0)}$ , and one odd, say  $\varphi_2^{(1)} = -\varphi_2^{(0)} + \pi$ , can be used in order to obtain any other by  $2\pi$  translations. Obviously, the phase cannot be determined other than mod  $2\pi$ .

To recapitulate briefly the foregoing considerations, we conclude that the state of the system is determined not only by the variables  $J, \varphi_1$  but also by the phase "quantum" number  $m$  which specifies how  $\varphi_1$  is being mapped into  $\varphi_2$ . Further on, we will use the term "state  $m$ " as an abbreviation for "the phase  $\varphi_2$  is given by  $\varphi_2^{(m)}$ " or "the phase  $\varphi_2$  is in the range  $\mathcal{R}_m$ ." Observe that Eq. (1), with its implied constraint  $J \leq I_1$ , can also be transcribed in a similar manner as Eq. (2') and a "quantum" number  $n$  for the driving phase  $\varphi_1$  can also be introduced. Shortly, we will apply such a transformation in another context, but there is no need to use it consistently because  $\varphi_1$  has no gaps in its range of allowed values.

We must ask now for the physical significance of the  $m$  states. The terminology, adopted here for lack of a better one, can lead to misunderstandings, which should be cleared up. Equation (2) specifies under what conditions the system can support the current  $J$  and be superconducting—and has no other meaning. The two junctions of the system are completely independent and only happen to be supplied by the same current. Therefore, the existence of the "forbidden" gap separating the  $m$  states does not mean that there is some restoring force keeping  $\varphi_2$  out of this region or that the second junction is physically compelled to occupy only one of the  $m$  states.

However, it is not difficult to point out situations in which some coupling between real, two-dimensional junctions would be established. It suffices to place the system composed of such junctions in nonuniform magnetic field to establish a constraint on the phase difference  $\varphi_1 - \varphi_2$ . Intergain junctions in high- $T_c$  materials can interact via the self-field of the feed current  $J$ , which can point in opposite directions on opposite grain sides. Another instance occurs when the system is included in a superconducting loop and the energy stored in the loop can provide the restoring torque. These remarks justify, to a certain extent, our usage of terms to which a purist may object.

Assuming, therefore, that in some circumstances different  $m$  states are accessible to the system it is legitimate to ask if transitions between these states can occur.

A proper answer to this question is beyond the scope of the present paper. It would require an investigation of the stability of solutions obtained after inclusion of the second Josephson equation (describing the time evolution of the phase) and inclusion of a specific coupling mechanism between junctions. Such an analysis is possible on the grounds of the resistivity shunted junction (RSJ) theory.<sup>7</sup> Nevertheless, a heuristic approach based on the examination of the system's energy in the limiting case of vanishingly small coupling energy can provide some useful hints.

## B. Energy-phase relations

Let us recall that the potential energy of a system containing only the first junction and the current source  $J$ ,

normalized to the Josephson coupling energy

$$E_0 = \frac{\Phi_0}{2\pi} I_1,$$

where  $\Phi_0$  is the flux quantum ( $\Phi_0 \cong 2.07 \times 10^{-15}$  Wb), is<sup>8</sup>

$$E_1(\varphi_1) = 1 - \cos\varphi_1 - j\varphi_1, \quad j = J/I_1. \quad (4)$$

A plot of this expression [see Fig. 1(a)] for a fixed value of  $J$  forms the popular washboard model of a Josephson junction. In this model, the junction behaves like a material point moving along the washboard. Such an object can occupy a stationary position either at the bottom of a valley or on the top of the ridge; the first state is stable, the second is metastable, no stable state is possible for  $J = I_1$ . The positions  $\varphi_{1n}$  of energy extrema are given by the roots of Eq. (1),

$$j = \sin\varphi_{1n},$$

i.e., are expressed by Eq. (2) after suitable substitutions. The energy barrier (normalized to  $E_0$ ) separating the successive extrema at  $\varphi_{1n}$  and  $\varphi_{1n+1}$  is (cf. Ref. 8)

$$\Delta E_1(\varphi_1) = 2(-1)^{n+1}[(1-j^2)^{1/2} + j\varphi_{10}] - j\pi, \quad (5)$$

where  $\varphi_{10}$  is the principal value of  $\arcsin j$ .

These observations allow us to use the energy-phase relations as an artifact to check on the stability of solutions and to visualize the evolution of the system disturbed out of equilibrium.

From Eq. (4) it is immediately seen that  $m$  states with even  $m$  correspond to valleys and those with odd  $m$  correspond to ridges in the potential energy of the second (driven) junction. One might suppose, therefore, that the odd states are always unstable. However, such a con-

clusion would be premature because we must consider the total energy of the system.

In the absence of interactions, the energy  $E_T$  of the whole system is just the sum of energies  $E_1$  and  $E_2$  of the individual junctions

$$E_T = E_1 + E_2.$$

By normalizing all energies to the Josephson coupling energy of the first junction, we obtain, after simple manipulations,

$$E_T(\varphi_1) = 1 - \cos\varphi_1 + \frac{1}{a}(1 - \cos\varphi_2) - j(\varphi_1 + \varphi_2). \quad (6)$$

Suppose now that even out of equilibrium the junctions remain phase-locked and  $\varphi_2$  is given by Eq. (2). Suppose further that the driving phase varies linearly over some interval encompassing several multiples of  $\pi$ . We can imagine that each time this phase crosses a  $\pi/2$  limit, the system has a choice between staying in the already occupied  $m$  state and making a transition into an adjacent state. In order not to complicate the issues, let us consider only two types of behavior. In type I the system will *always* make a transition from  $m$  to  $m \pm 1$ , the sign depending on whether the phase  $\varphi_1$  increases or decreases its value at the transition point. In other words, in type-I behavior,  $\varphi_2$  tries to linearly follow the driving phase. In type-II behavior, the system will *always* stay in one state and  $\varphi_2$  will change periodically with  $\varphi_1$ .

From Eq. (6) we obtain, for the energy barrier  $\Delta E_T$  separating the successive extrema of total energy in type-I behavior,

$$\Delta E_{T(I)} = \Delta E_1 + \Delta E_2, \quad (7a)$$

where  $\Delta E_1$  is given by Eq. (5), and  $\Delta E_2$  by its equivalent for the second junction:

$$\Delta E_2(\varphi_2) = 2(-1)^{m+1}[a^{-1}(1-j^2a^2)^{1/2} + j\varphi_{20}] + j\pi,$$

where  $\varphi_{20}$  is the principal value of  $\arcsin(aj)$ , i.e., in consistent notation  $\varphi_{20} = \varphi_2^{(0)}(\varphi_{10})$ . In type-II behavior we have

$$\Delta E_{T(II)} = \Delta E_1 - \Delta E_2 + 2j\pi. \quad (7b)$$

In the special case  $a = 1$ , as already discussed, there are no gaps between the  $\mathcal{R}_m$  ranges and all values of  $\varphi_2$  are allowed. Type-I behavior simply means  $\varphi_2 = \varphi_1$  and, consequently,  $E_1 = E_2$ ,  $E_T = 2E_1$ , and  $\Delta E_T = 2\Delta E_1$ . This case is shown in Figs. 1(a) and 1(b) for  $j = 0.6$ . In Fig. 1(a) we show  $E_2$  (normalized additionally to  $2\pi$ , solid line) and  $\varphi_2$  (dashed line) versus  $\varphi_1$ , and in Fig. 1(b) the corresponding plot of  $E_T(\varphi_1)$ , normalized in the same manner. For convenience we have kept  $j = 0.6$  throughout all examples shown in Figs. 1 and 2, and thus Fig. 1(a) can always be referred to as the plot of  $E_1(\varphi_1)$ .

While in the type-I regime, the system behaves like a single junction, type-II behavior produces more interesting effects. Let us assume that the system stays put in the  $m = 0$  state and let  $\varphi_1$  be in the  $[-\pi/2, \pi/2]$  interval ( $n = 0$ ). Then,  $\varphi_2 = \varphi_0 = \varphi_1$  and we have, in this interval,  $E_1 = E_2$ , as in the previous case. However, if  $\varphi_1$  moves to the next interval, for instance,  $[\pi/2, \pi + \pi/2]$  or  $n = 1$ ,

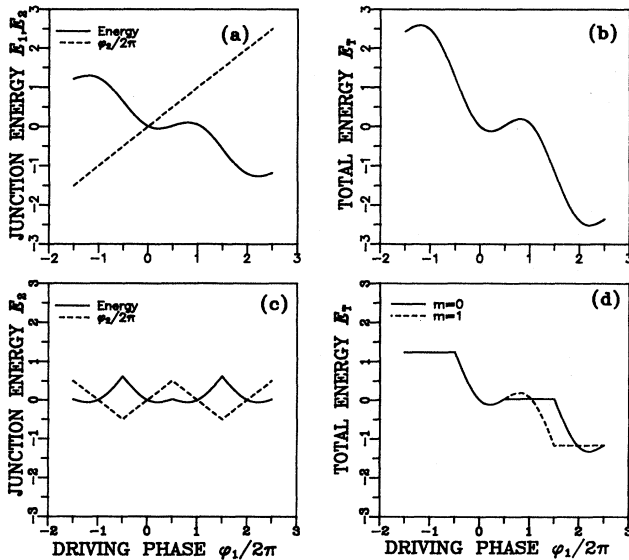


FIG. 1. Energy-phase diagrams for a series array of two identical junctions. Type-I behavior: (a) and (b), type-II behavior: (c) and (d). Energies are normalized to the Josephson coupling energy  $E_0/2\pi$ .

then  $\varphi_2 = \varphi_2^{(0)} = \pi - \varphi_1$ . Upon substitution of this value into Eq. (6), we get constant energy

$$E_T = -\pi j .$$

Type-II behavior for  $a = 1$ ,  $m = 0$  is illustrated in Figs. 1(c) and 1(d). As seen, the ridges in the total-energy diagram of Fig. 1(d) are obliterated and the height of the energy barrier separating the equilibrium position at a valley bottom from the next energy extremum is halved. The system, excited from equilibrium to the metastable state represented by the plateau, could be trapped there for an infinite time.

An interesting variation of the plateau effect occurs in type-II behavior if we assume that the permanently occupied  $m$  state is even. In this case, not the ridges but the valleys are obliterated, as shown by the dashed curve in Fig. 1(d), and the system, escaping from one metastable position at the top of a ridge, finds itself in another of the same kind on a plateau; one might say it is a reminder of the inherent metastability of even- $m$  states.

However, it can be easily shown for  $a = 1$  that the beginning of each plateau in the energy level of state  $m$  is the branching point of the energy level corresponding to state  $m + 1$  and that the latter crosses the plateau at its middle point. Reciprocally, the plateau due to state  $m + 1$  is crossed by the "riser" of state  $m$  [see Fig. 1(d)]. The system which was driven by an excitation to a plateau has, therefore, the means of relaxation to a stable equilibrium position. It can relax either by reverting to type-I behavior at the branching point or making a transition to the  $m + 1$  state at the crossing point. Moreover, it is seen that  $E_T(\varphi_1)$  becomes multivalued and hysteretic response to excitations is possible.

Another distinguishing feature of type-II behavior is the discontinuity in the derivative of  $\varphi_2$  with respect to  $\varphi_1$  [see Fig. 1(c)] occurring at the limits of each range  $\mathcal{R}_m$  and reflected in the energy-phase relations.

We conclude that, with no other constraints imposed, a single-connected system in the degenerate case  $I_1 = I_2$  can exhibit either type-I or type-II behavior, with possible departures from type II at the crossing points of energy levels. Type II is more probable because it encounters lower-energy barriers at the branching points. The choice between type I and II will be made at the branching point and, in a real system, will be determined by the parameters which do not appear in our model: the junction(s) self-inductance, capacitance and normal-state resistance, as well as by the coupling energy.

The condition  $I_1 = I_2$  cannot really be fulfilled by any physical system. Let us consider now the more realistic case  $a < 1$ . Type-I behavior in this case is hindered by the existence of gaps in the allowed ranges of  $\varphi_2$  values which translate into energy barriers separating individual  $m$  states. The height of the barrier between states  $m$  and  $m + 1$  is given by the expression

$$\Delta E_{\text{gap}} = 2[(-1)^{m+1} a^{-1}(1-a^2)^{1/2} + 2j\Psi] , \quad (8)$$

where  $\Psi$  is given by Eq. (2a).

The energy-phase diagrams that would result if some mechanism inducing transitions across energy barriers

were available and thus type-I behavior enabled, are shown in Figs. 2(a) and 2(b) for the case of  $j = 0.6$  and  $a = 0.8$ .

The energy barriers will tend to establish type-II behavior as the only permissible behavior. Figures 1(c) and 1(d) illustrate such behavior for  $m = 0$  and previous values of the other parameters. In comparison with the previously considered case of equal critical currents, we note in Fig. 2(c) that  $E_2$  and  $\varphi_2$  are now smooth functions of  $\varphi_1$ , and in Fig. 2(d) that the plateaus in the plot of total energy now have nonzero curvature. The latter fact indicates that the lifetime of the system in the metastable state will be longer than for a single junction, but finite.

For  $m$  odd the system will now find a shallow depression in the plateau for its equilibrium position. This is shown in Fig. 2(d) by the dashed curve ( $m = 1$ ). We note that, for the particular values of  $a$  and  $j$  chosen for the plots in Fig. 2, the crossing energy levels allow the system to pursue a continuous evolution path which avoids the phase gaps. It can be shown that the overlap in energy levels occurs only for

$$aj \geq \frac{2}{\pi}$$

or

$$a = 1 .$$

If  $a$  exceeds the critical value  $a_0 = 2/\pi$ , then (assuming that  $j$  does not instantaneously change its sign) the transitions between  $m$  states can occur only across the gap, to which, in this case, from Eq. (8), corresponds an energy barrier  $\Delta E_{\text{gap}} \approx 3.5E_0$ . In such a situation, the system

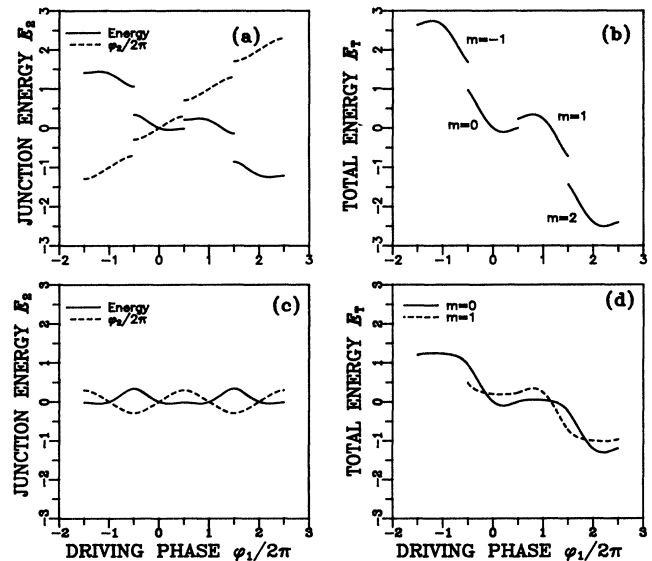


FIG. 2. Energy-phase diagrams for a series array of two different junctions (critical current ratio  $a = 0.8$ ). Type-I behavior: (a) and (b), type-II behavior: (c) and (d). Energies are normalized to the Josephson coupling energy of the first junction  $E_0/2\pi$ .

once excited to an odd- $m$  state will be permanently trapped there (in the absence of a restoring mechanism).

### C. Phase-reversal transitions

We return now to the problem of transitions between adjacent  $m$  states. In the foregoing discussion we have, more or less, tacitly assumed the occurrence of such transitions and have shown that, in certain cases, the occupation of odd- $m$  states lowers the potential energy of the system.

In the system we have been considering so far, the stationary  $m$  states cannot be associated with any directly observable quantity. In the absence of any particular coupling mechanism, the transitions are purely formal concepts involving phase reversal and a slip of  $\pi$ :  $\varphi_2 \Rightarrow -\varphi_2 + \pi$ . This transformation, which conserves the current flowing in the system, at the gap edge advances  $\varphi_2$  for the gap width  $2\Psi$ , and at the crossing point of energy levels is reduced to a  $\pi$  shift. It is tempting to consider a "phase-flip" process in which both phases simultaneously undergo such transformations with opposite signs of  $\pi$  shifts but, so far, there is no need for it.

Transitions occurring at the gap edge directly change the system's energy while crossing-point transitions apparently conserve it, but, in fact, both require an initial energy to drive the system out of equilibrium, so that the total-energy change will be given always by Eq. (7). If the equilibrium position is already at the gap edge ( $j \approx 1$ ), then the stability of the system is greatly reduced ( $\Delta E_T \approx 0$ ) and a small fluctuation of  $j$  can drive the weakest function of the system normal.

From the physical point of view, the occurrence of a transition whose path leads directly across the gap means that the driving junction stays normal only momentarily and returns to the superconducting state after rearrangement of the driven phase. It is the recovery process that requires the presence of some restoring torque. Under no circumstances can the driven junction, of higher critical current, cross the phase gap without first pulling the weaker driving junction into the resistive state. As a consequence, when the system is dissipative for time-dependent processes, the transition might be detected by the accompanying voltage pulse across the junction array.

For very narrow gaps ( $a \approx 1$ ), macroscopic quantum tunneling cannot be excluded as a probable nondissipative mechanism enabling transitions. As to the dissipative transitions, we can evoke the analogy to the phase-slip process occurring in long Josephson weak links. Both on the grounds of time-dependent superconductivity<sup>9</sup> and in the RSJ model,<sup>10</sup> this dissipative process is explained as a transient destruction of the superconducting order followed by its restoration.

After these generalities, let us consider a specific case in which the restoration mechanism is well established. The system will be no more single connected. Assume that our array of two different junctions is shunted by some finite superconducting inductance  $L$  and that the resulting loop is linked by magnetic flux  $\Phi$ . The source current  $J$  for each value of  $\Phi$  will be then divided in some

stable manner between the junction array and the inductive shunt. The junctions' phases and the flux will then fulfill the fluxoid equation

$$2\pi\Phi = \varphi_1 + \varphi_2 + 2\pi k, \quad (9)$$

where  $\Phi$  is expressed in units of  $\Phi_0$  and  $k$  is an integer. Equation (9) imposes a new constraint on  $\varphi_1$  and  $\varphi_2$ , which still have to satisfy the current continuity relation (2).

Let us assume now that, for some value  $\Phi = \Phi_{\text{gap}}^-$ , the current through the junctions is very close to the critical current of the first junction. We know that in this situation

$$\varphi_1^- = \pi/2, \quad \varphi_2^- = \pi/2 - \Psi = \varphi_2^{(0)},$$

and, from Eq. (9),

$$2\pi\Phi_{\text{gap}}^- = \pi - \Psi + 2\pi k.$$

Let us now increase, in a time short with respect to the time constant,  $\tau = L/R_n$ , where  $R_n$  is the normal-state resistance of the driving junction, the flux  $\Phi$  to a new value  $\Phi_{\text{gap}}^+$  such that

$$2\pi\Phi_{\text{gap}}^+ = \pi + \Psi + 2\pi k.$$

It is seen immediately that the only acceptable solution of Eq. (9) in this new situation, preserving the previous current distribution (hence, the magnetic energy stored in the system), is

$$\varphi_1^+ = \pi/2, \quad \varphi_2^+ = \pi/2 + \Psi = \varphi_2^{(1)}.$$

The other solution

$$\varphi_1 = 3\pi/2, \quad \varphi_2 = -\pi/2 + \Psi = \varphi_2^{(0)},$$

must be rejected because it means reversal of the current through the junction array.

As seen, the acceptable solution involves an  $m \rightarrow m + 1$  transition. Can the system execute it? The answer is positive. The only alternative to the transition is that the driving junction, in an attempt of the system to adjust the phases continuously, will go normal. As a consequence, the current will be expelled from the junction array. However, that means reestablishment of the superconducting order in the array, hence, in the whole system. Equation (9) can now take hold again and enforce the required phase distribution.

Now, let us see what happens if we do not jump the gap but proceed slowly. Let the new flux value be  $\Phi_{\text{gap}}$  such that

$$2\pi\Phi_{\text{gap}} = \pi.$$

Since  $\varphi_2 = \pi/2$  is excluded, there are now two equivalent (also in energy) solutions of Eq. (9):

$$\varphi_1 = \pi, \quad \varphi_2 = 0 = \varphi_2^{(0)},$$

and

$$\varphi_1 = 0, \quad \varphi_2 = \pi = \varphi_2^{(1)}.$$

Both solutions correspond to current expulsion from the

array. The bifurcation starts as soon as the flux  $\Phi$  increases infinitesimally from  $\Phi_{\text{gap}}^-$  (or decreases from  $\Phi_{\text{gap}}^+$ ) and can be accompanied by additional instabilities, depending on the gap width.

Now, current expulsion at flux values equal to odd multiples of a half-flux quantum would also happen if the system contained only a single junction, and one may suspect that we are discussing a not particularly interesting effect. To show the contrary, let us consider the case  $j=0$ , i.e., limit our interest to a rf SQUID configuration. Applying the external flux  $\Phi_e$  to the system, we induce a persistent current  $-I_1 \sin \varphi_1$ , and the total flux  $\Phi$  appearing in Eq. (9) is<sup>8</sup>

$$\Phi = \Phi_e - (\beta/2\pi) \sin \varphi_1, \quad \beta = 2\pi L I_1.$$

Using Eq. (9) in the standard manner<sup>8</sup> to evaluate  $\varphi_1$  and Eq. (2) to eliminate  $\varphi_2$ , we arrive at the equation

$$\Phi_e = \Phi + (\beta/2\pi) \frac{\sin 2\pi\Phi}{(1 + 2a \cos 2\pi\Phi + a^2)^{1/2}}, \quad (10)$$

which, for  $a=0$ , is reduced to the usual transcendental equation appearing in rf SQUID theory.

Equation (10) has several interesting features, its geometrical interpretation included. It is invariant under the transformation  $\varphi_2 = -\varphi_2 + \pi$ , i.e., it does not depend on whether the junction array assumes type-I behavior or not. In general, it predicts an enhanced nonlinear response of the SQUID to the applied flux and an apparent increase of the effective inductance. The critical value of the  $\beta$  parameter,  $\beta_c$ , which sets the limit for multivalued  $\Phi(\Phi_e)$  dependence (i.e., dissipative SQUID regime), depends strongly on  $a$  and, for  $0 < a < 1$ ,  $\beta_c < 1$ . As an example, for the array shown in Fig. 2 ( $a=0.8$ ),  $\beta_c \approx 0.217$ .

The analysis becomes slightly complicated as  $a$  approaches unity, Equation (10) takes then the form

$$\Phi_e = \Phi \pm \beta (2\pi\sqrt{a})^{-1} \sin \pi\Phi, \quad (10')$$

where the sign is that of  $\cos 2\pi\Phi$ . If we had substituted, for  $a=1$ , the solution  $\varphi_2 = \varphi_1$  directly into Eq. (10), omitting  $\varphi_2 = \pi - \varphi_1$ , we would have obtained the erroneous result

$$\Phi_e = \Phi + (\beta/2\pi) \sin \pi\Phi.$$

Now  $\beta_c$  is determined from the condition that, for  $\beta \geq \beta_c$ , the slope  $d\Phi/d\Phi_e$  can go to infinity.<sup>4</sup> Equation (10') involves a discontinuity in  $d\Phi_e/d\Phi$  at  $\Phi = (2k+1)/2$  (in units of  $\Phi_0$ ) and this condition can be met for any value of  $\beta$ . In other words,  $\beta_c \rightarrow 0$  for  $a \rightarrow 1$ . In rf SQUID applications it means that the device containing a degenerate junction array will always be dissipative.

From our point of view,  $\beta > \beta_c$  means that the gap-edge transitions will be enforced independently of the flux slew rate. For SQUID's intended to operate in the dissipative mode, this effect will not be particularly detrimental and an observer unaware of the presence of a "hidden" series junction will notice only an increased effective inductance.

However, Eq. (10') has consequences not limited to the

SQUID operation. Let us observe first that, in the vicinity of singular points  $\Phi_k = (2k+1)/2$ ,  $\Phi$  is a multivalued function of  $\Phi_e$ . This is shown by substituting  $\Phi = \Phi_k + \delta$  and  $\Phi_e = \Phi_k + \delta_e$  into Eq. (10'). We then obtain

$$\delta_e = \delta \pm \beta' \cos \delta, \quad \beta' = \beta (2\pi\sqrt{a})^{-1}$$

and for  $\delta \ll 1$  the solution is  $\delta \approx \delta_e \mp \beta'$ . The energy of the junction array is clearly on a plateau as in Fig. 1(a) (for  $J=0$ ), and for the energy of the whole system this plateau is modified only by the magnetic interaction energy<sup>8</sup> (expressed in units of  $E_0$ )

$$E_M = \frac{2\pi}{\sqrt{a}\beta'} [2\pi\Phi_e - (\varphi_1 - \varphi_2)]^2 \approx \frac{2\pi}{\sqrt{a}\beta'} (\delta_e \mp \beta')^2.$$

As is seen,  $\beta'$  plays the role of the surrogate phase gap and is associated with an energy barrier which, in this linear approximation, will be proportional to  $\beta'$  if we assume that the approximation is valid up to some  $\delta_{e\text{max}} \propto \beta'$ .

It follows from the above considerations that even a very weakly inductively coupled series array of degenerate junctions, dc biased or not, will respond to the passage of flux quantum by transitions in and out of the  $m=1$  state. This is a potential source of noise in systems not intended for use as rf SQUID's. For sufficiently slow flux changes, these transitions would be separated in time by intervals of the order of  $L/R_n$ . This picture is not inconsistent with the telegraphlike noise observed in granular high- $T_c$  thin films.<sup>11,12</sup>

### III. CRITICAL CURRENT OF SERIES-PARALLEL ARRAYS

#### A. Analytical results

As a generalization of the multiple connected system introduced in Sec. II C, let us consider the circuit, shown schematically in Fig. 3. Each of the two parallel branches of the circuit is formed by a series inductance  $L_n$ ,  $n=1,2$  and a series array of  $N_n$  junctions. The junctions are characterized by their critical currents

$$I_{ni}, \quad i=1,2, \dots, N_n, \quad n=1,2$$

and superconducting phase differences, denoted  $\varphi_{ni}$ . The object of interest is now the maximal value  $J_{\text{max}}$  of the dc current  $J$  which can be passed through the circuit in the presence of the magnetic flux  $\Phi$ .  $J_{\text{max}}$  will be called the critical current of the circuit.

Without any loss of generality it can be assumed that the junctions in each branch are numbered in ascending order of the values of the relevant critical currents, i.e.,

$$I_{ni} \leq I_{ni+1} \quad (11)$$

and also that

$$I_1 \leq I_2, \quad (12)$$

where  $I_n \equiv I_{n1}$ . In what follows, the index  $n$  will refer to the branch number and the index  $i$  to the junction number under the convention given by Eqs. (11) and (12).

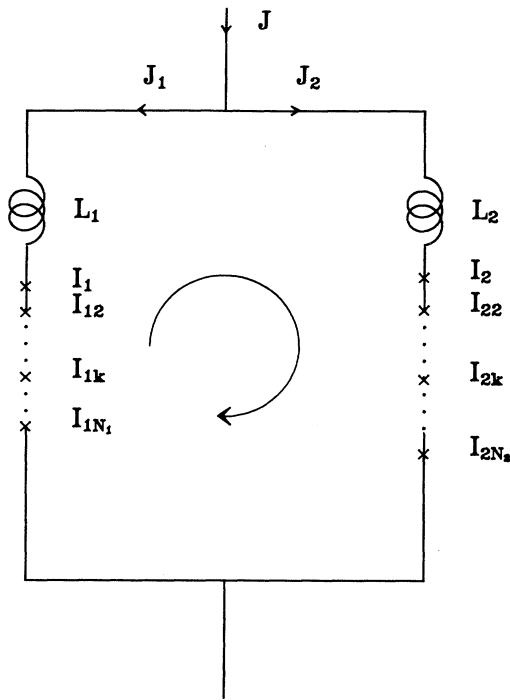


FIG. 3. Schematic representation of the circuit considered in the text. Crosses indicate Josephson junctions, labeled by their critical currents. The arrow in the center indicates the direction of fluxoid integration path.

The total current  $J$  is the sum of currents  $J_n$  in the individual branches

$$J = J_1 + J_2 \quad (13)$$

and the latter must obey the Josephson relations

$$J_n = I_{ni} \sin \varphi_{ni} \quad (14)$$

In an obvious generalization of the procedure used in the preceding section, we define the quantities

$$a_{ni} = I_n / I_{ni} \leq 1 \quad (15a)$$

and

$$\psi_{ni} = \arccos a_{ni}, \quad 0 \leq \psi_{ni} \leq \pi/2 \quad (15b)$$

The general solutions of Eq. (14) for  $i > 1$  can now be expressed as functions of the driving phases

$$\varphi_{ni} \equiv \varphi_n$$

(note that  $\varphi_2$  now has a different meaning from  $\varphi_2$  of the preceding section),

$$\varphi_{ni} = \varphi_{ni}^{(m)} = (-1)^m \varphi_{ni}^{(0)} + m\pi, \quad (16)$$

where

$$\varphi_{ni}^{(0)} = \arcsin(a_{ni} \sin \varphi_n), \quad \varphi_{ni}^{(0)} \in \mathcal{R}_{ni}^0 \quad (17)$$

and

$$\mathcal{R}_{ni}^0 = (\pi/2 + \Psi_{ni}, \pi/2 - \Psi_{ni}).$$

The considered system is subject to the constraint imposed by the fluxoid conservation relationship which can be written as

$$\sum_{n,i} \text{sgn}(n) \varphi_{ni} + 2\pi\Phi = 2k\pi, \quad (18)$$

where  $k$  is an integer,  $\Phi$  is expressed again in units of  $\Phi_0$ , and  $\text{sgn}(n) = \pm 1$ , the  $+$  sign occurring when the directions of the fluxoid integration and current paths coincide over branch  $n$ —this notation is convenient when more than two parallel branches are considered. In the conventions shown in Fig. 3,

$$\text{sgn}(1) = -1$$

and

$$\text{sgn}(2) = 1.$$

It is now necessary to explicitly take into account the contribution  $\Phi_i$  made to the total flux  $\Phi$  by the inductances

$$\Phi_i = \sum_n \text{sgn}(n) L_n J_n, \quad (19)$$

where  $L_n$  has the dimension of inductance  $\Phi_0$ , and to express the total flux  $\Phi$  as the sum of  $\Phi_i$  and the externally applied flux  $\Phi_e$

$$\Phi = \Phi_i + \Phi_e. \quad (20)$$

Upon substitution of (19), (20), and (14), Eq. (18) takes its final form

$$F(\varphi_1, \varphi_2) = \sum_{n,i} \text{sgn}(n) \varphi_{ni} + 2\pi \sum_n \text{sgn}(n) L_n J_n + 2\pi\Phi_e - 2\pi k = 0, \quad (21)$$

where  $\Phi_e$  is considered to be a parameter.

The problem of maximizing the current  $J$  through a two-junction interferometer was routinely handled using the technique of Lagrange multipliers.<sup>13</sup> However, the problems with constraints given in the form of Eq. (21) do not really need this method. Observe that Eq. (21), together with current continuity relations (13) and (14), institutes a functional dependence  $\varphi_2(\varphi_1)$ , and, in order to maximize  $J$ , it suffices to solve the equation

$$\frac{dJ}{d\varphi_1} = I_1 \cos \varphi_1 + I_2 \cos \varphi_2 \frac{d\varphi_2}{d\varphi_1} = 0, \quad (22)$$

rejecting the trivial solution  $d\varphi_2/d\varphi_1 = 0$ . No special notation is introduced, but it is to be understood that Eq. (22) occurs at some specific values of  $\varphi_1$  and  $\varphi_2$ .

From Eq. (21) we immediately obtain

$$\frac{d\varphi_2}{d\varphi_1} = - \frac{\partial F}{\partial \varphi_1} \left[ \frac{\partial F}{\partial \varphi_2} \right]^{-1}.$$

Partial derivatives in the above expression involve terms of the form  $d\varphi_{ni}/d\varphi_n$ . Substitution of  $\varphi_{ni}$  from Eq. (16) evaluates these terms to

$$a_{ni} \cos \varphi_n / \cos \varphi_{ni}^{(m)} = (-1)^m a_{ni} \cos \varphi_n / (1 - a_{ni}^2 \sin^2 \varphi_n)^{1/2}.$$

With the help of this observation, and taking into account that each junction “ $ni$ ,”  $i \geq 2$  can be in a different state  $m_{ni}$ , we can write

$$\frac{d\varphi_2}{d\varphi_1} = \frac{1 + \beta_1 \cos \varphi_1}{1 + \beta_2 \cos \varphi_2}, \quad (23)$$

where

$$\beta_n = \beta_n^{(m)}(\varphi_n) = \alpha_n^{(m)}(\varphi_n) + 2\pi L_n I_n \quad (24)$$

and

$$\alpha_n^{(m)}(\varphi_n) = \sum_{i=2}^{N_n} \frac{a_{ni}}{(1 - (-1)^{m_{ni}} a_{ni}^2 \sin^2 \varphi_n)^{1/2}}. \quad (25)$$

The singularity in  $\alpha_n^{(m)}$ , occurring at  $\varphi_n = \pm k\pi$ , corresponds to the earlier rejected trivial solutions  $d\varphi_2/d\varphi_1 = 0$ .

Equation (22) is now reduced to

$$\frac{I_1 \cos \varphi_1}{1 + \beta_1 \cos \varphi_1} = \frac{I_2 \cos \varphi_2}{1 + \beta_2 \cos \varphi_2}. \quad (26)$$

Note that, for  $N_n = 1$ , the expression for  $\beta_n$  is reduced to  $\beta_n = 2\pi L_n I_n = \beta_{0n}$  and, if both branches hold only one junction, Eq. (26) becomes the well-known result of the two-junction interferometer theory.<sup>19</sup> The technique of using such an equation to construct the  $J_{\max}(\Phi_e)$  or  $\Phi(\Phi_e)$  plots is well explained in Ref. 14.

Briefly, Eq. (26) allows us to calculate, for a given set of  $m_{ni}$  states and for a given  $\varphi_1$  from some fixed interval (of length  $\geq \pi$ ), the corresponding value (or values) of  $\varphi_2$ , limited to some other (or the same) interval. In this manner, a sufficient number of  $(\varphi_1, \varphi_2)$  pairs can be obtained and these, upon substitution to Eqs. (13), (16), and (21) yield the other relevant parameters. The task is facilitated by the fact that Eq. (26) is even in both  $\varphi_1$  and  $\varphi_2$ , and thus, if it is satisfied by  $(\varphi_1, \varphi_2)$ , then the same can be said of  $(\pm\varphi_1, \pm\varphi_2)$  in any combination of signs.

## B. Numerical results and discussion

Figures 4–8 were drawn using the above-described method. Before discussing them in more detail, let us draw attention to some analytical features of Eq. (26). The conclusions drawn in earlier work for the two-junction case mostly retain their validity, e.g., those concerning the stability of solutions, as discussed by Peterson and Hamilton,<sup>14</sup> and we will not dwell upon them. For instance, if the “additional” junctions are very strong ( $a_{ni} \ll 1$ ,  $i \geq 2$ ), the denominator in (25) can be neglected and the only effect for all  $m_{ni} = 0$  will be the effective increase of inductances  $L_n$  by the addition of the terms  $\sum_{n,i} (I_{ni})^{-1}$ .

One should not, however, be left with the impression that nothing is really changed in comparison to the two-junction interferometer. Consider the case of each

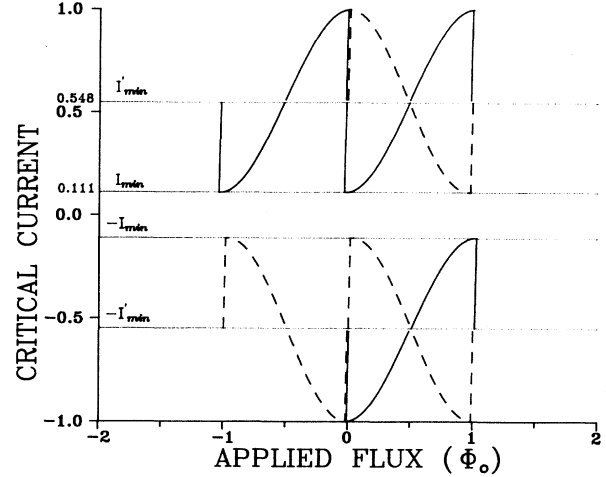


FIG. 4. Critical current (normalized to  $I_{\max} = I_1 + I_2$ ) vs applied flux (in units of  $\Phi_0$ ) for the circuit shown in Fig. 3 with  $N_1 = N_2 = 2$  and  $I_1 = I_{12} = 0.8$ ,  $I_2 = I_{22} = 1.0$  ( $a_{ni} = 1$ ),  $\beta_{01} = \beta_{02} = 1$ . Solid lines represent the (0;0) solution with both circuit branches in the  $m = 0$  state (phases of junctions “12” and “22” limited to the  $[-\pi/2, \pi/2]$  interval), dashed lines represent the (1;1) solution with both branches in  $m = 1$  state (phases of junctions “12” and “22” taken from the  $[\pi/2, 3\pi/2]$  interval). Both solutions are  $\Phi_0$  periodic and their overlap produces a critical current modulation between  $I_{\max}$  and  $I'_{\min}$ .

branch containing  $N$  identical junctions. Equation (26) then becomes

$$\frac{I_1 \cos \varphi_1}{N + \beta_{01} \cos \varphi_1} = \frac{I_2 \cos \varphi_2}{N + \beta_{02} \cos \varphi_2} \quad (\beta_{0n} = 2\pi L_n I_n). \quad (27)$$

Apparently, this is the formula for a two-junction interferometer with the  $\beta$ 's  $N$ -fold reduced, contrary to the expectation that the inductive behavior would be enhanced. A quick reference to the fluxoid equation (18) produces an even more bewildering result. The phases of all junctions in a given branch can be assumed to be identical (type-I behavior) and Eq. (18) takes the form

$$\varphi_2 - \varphi_1 = 2\pi \left[ \frac{k}{N} - \frac{\Phi}{N} \right],$$

i.e., predicts a flux period of  $N\Phi_0$ . This is the same problem we have dealt with in conjunction with Eq. (10) and the rf SQUID configuration, but here it is resolved differently.

It is true that the fundamental “ace of diamonds” pattern of critical current versus applied flux (see Fig. 4) has a periodicity of  $N\Phi_0$  and, if normalized to this single period, it has the same shape as its two-junction analogue. This is shown in Fig. 4 for the case  $N = 2$ . However, the fluxoid is *always*  $\Phi_0$  periodic and the fundamental pattern is reproduced every  $\Phi_0$ . It is the envelop of such intersecting patterns which finally gives the critical current dependence on the applied flux. As seen in Fig.



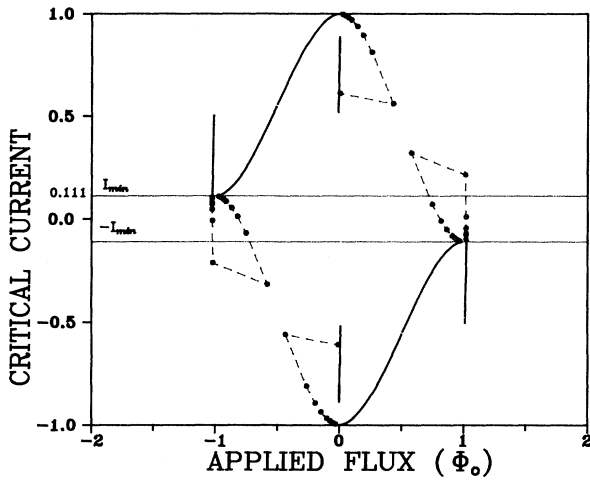


FIG. 5. Normalized critical current vs applied flux for the circuit parameters as in Fig. 4, except that the critical currents are now slightly different:  $I_{12}=0.808$ ,  $I_{22}=1.01$  ( $a_{ni}=0.99$ ). The solution (0;0), with both circuit branches in the  $m=0$  state, is shown. Dashes join the points, computed with the same increment of the driving phase as the solid lines and mark the unstable branches of the solution.

4, the current will oscillate between  $I_{\max}=I_1+I_2$  and some value  $I'_{\min} > I_{\min}$ , where  $I_{\min}=I_2-I_1$  is the “expectation value” for the minimal critical current.

The nearly vertical slashes seen in Fig. 4 at integer multiples of  $\Phi_0$  are characteristic for the case of (nearly) degenerate arrays and  $N_1=N_2$ . Suppose that  $\varphi_1$  and  $\varphi_2$  satisfy Eq. (26) for the same parameters as those used to plot Fig. 4, except  $\beta_{01}=\beta_{02}=0$ . Hence,  $\varphi_1$  and  $\varphi_2$  are the phases across the first junction in each branch. Suppose further that the second junctions are both in the  $\varphi^1$  state, i.e., their phases are given by  $\pi-\varphi_1$  and  $\pi-\varphi_2$ , respectively. After substitution of these values into Eq. (21), it

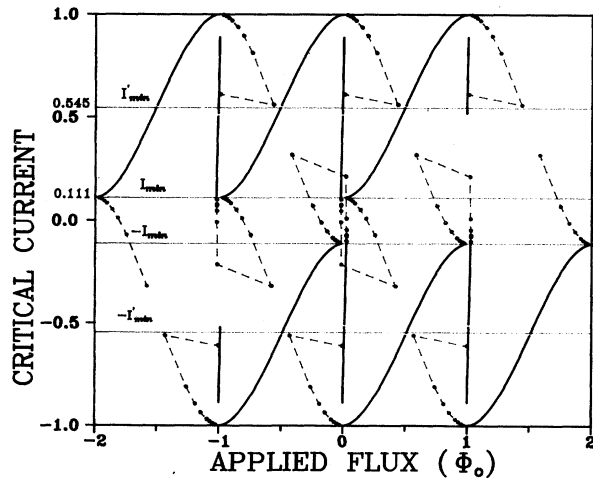


FIG. 6. Critical current pattern in Fig. 5 reproduced periodically in order to show the overlap resulting in the critical current modulation by the applied flux. The overlap is not complete if only the (0;0) solution is used.

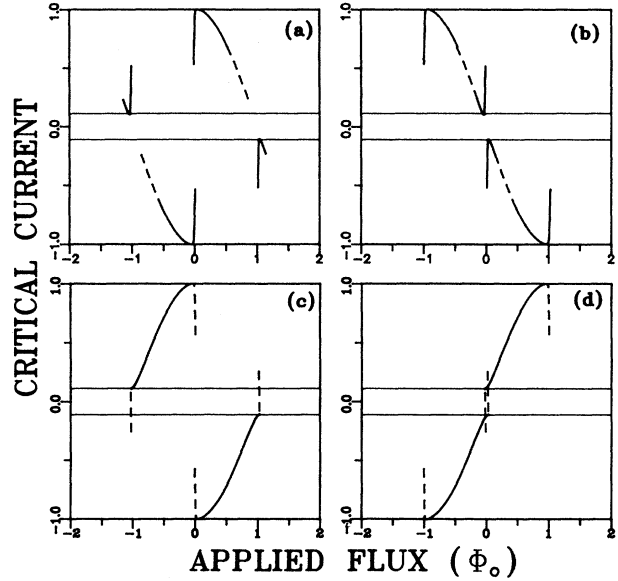


FIG. 7. Normalized critical current vs applied flux for the circuit parameters as in Fig. 5 and for different  $m$  states of the circuit branches: (a),  $(-1;0)$ ; (b)  $(1,0)$ ; (c)  $(0;-1)$ ; and (d)  $(0,1)$ . Dashes indicate unstable branches and horizontal solid lines represent the  $\pm I_{\min}$  limits.

is seen that  $\varphi_1$  and  $\varphi_2$  disappear completely from the phase balance and only the requirement  $\Phi_e=k\Phi_0$  is left.<sup>15</sup> The resultant vertical slash in the  $J(\Phi_e)$  pattern becomes slightly inclined when  $0 < \beta_n^0 \ll 1$ , as is the case in Fig. 4.

Figures 5–8 are related to a slightly modified situation: the “ $n1$ ” junctions are the same as before but the “ $n2$ ” have critical currents 1% higher, i.e.,  $I_{12}=0.808$  and

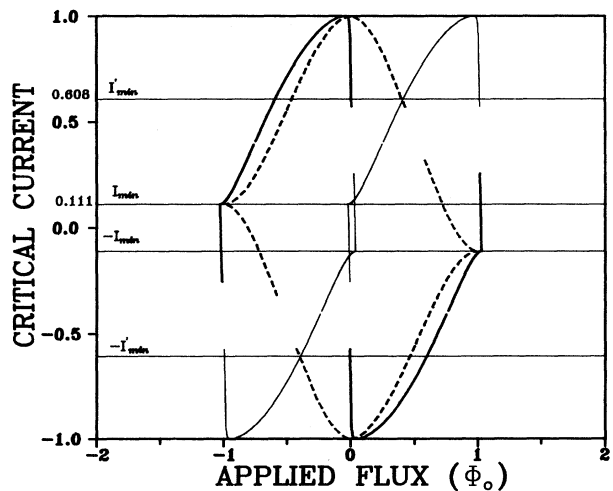


FIG. 8. The outline of the (0;0) pattern from Fig. 5 (short dashes) plotted together with the (0;-1) pattern from Fig. 7(c). The next period of the (0;-1) pattern is also reproduced (thin solid line) in order to indicate the overlap. This construction demonstrates that the critical current is a multivalued function of applied flux in the envelop region.

$I_{22} = 1.01$ , or  $a_{ni} = 0.99$ . The  $\varphi_{n2}^{(1)}$  states are now separated by gaps from the corresponding  $\varphi^{(0)}$  states.

In Fig. 5 we show the fundamental “ace of diamonds” pattern obtained by admitting only  $m = 0$  states, and, in Fig. 6, the same pattern is reproduced periodically in order to show the overlap which changes the minimal critical current. The circles on the dashed curves (which correspond to  $\varphi_2$  in the  $\mathcal{R}_1$  range) represent the actual computation points obtained from Eq. (26) with the same increment of  $\varphi_1$  as for the solid curves and their density is a measure of the rate of change of  $\varphi_2$  with  $\varphi_1$ , or—in a sense—a measure of the stability of this solution. Observe that the solutions now enter the  $(-I_{\min}, I_{\min})$  region—clearly a consequence of the gap effect—and that the overlap in Fig. 6 is not complete, because an incomplete set of  $m$  states was employed.

If we introduce the notation  $(m_1; m_2)$  to summarily designate the state of the driven junctions in each branch of the system which contains only two such junctions, then Figs. 5 and 6 relate to  $(0; 0)$ . In Figs. 7(a)–7(d) we show the critical current versus applied flux for  $(1, 0)$ ,  $(-1, 0)$ ,  $(0, -1)$ , and  $(0, 1)$ , respectively. This presentation is obviously redundant since  $(\pm m_1; m_2)$  plots can be obtained from each other by the  $\Phi_0$  translation, but in this manner the details of each plot and their mutual relations can be better displayed.

In Fig. 8 we have brought together the outline of the  $(0; 0)$  pattern from Fig. 5 (marked by short dashes) and the  $(0; -1)$  pattern from Fig. 7(c). Part of the next period of the  $(0; -1)$  pattern—or of  $(0; 1)$  from Fig. 7(d), which is the same—is also reproduced in order to indicate the overlap. This construction was plotted to demonstrate several points, all related to the existence of phase gaps

(1) The higher states can occupy the free space above the envelop determined by the lower states and thus they can further reduce the depth of modulation of the critical current by the applied flux.

(2) The higher states can form separate peaks in the envelop space (not very well resolved in Fig. 8 because of the small gaps) and thus produce a spurious modulation.

(3) Critical current is nearly everywhere a multivalued function of the applied flux and even small phase gaps, i.e., small differences in the critical currents of component junctions, produce significant variations in this function. This must be a source of instabilities in the response to the applied flux.

In general, it seems that, for a system composed of different junctions, the ensemble of available states on the  $(J_{\max}, \Phi_e)$  plane forms a continuous contour having multi-

ple intersection points. Such points always exist close to the extremes of the envelop. It appears, therefore, that in the course of its evolution in the applied flux, the system is able to cross from any initial state to any other state. Further study is needed to determine the energy levels corresponding to the various states and to identify the regions of possible across-the-gap transitions.

#### IV. CONCLUSIONS

The inclusion of series junctions into a superconducting inductive loop is shown to enhance its hysteretical behavior. In the rf SQUID configuration (without applied current bias) and in the limiting case of identical junctions, the relation between the flux in the loop and the applied flux is always multivalued, independently of the loop inductance. Such loops in granular high- $T_c$  material would constitute an additional noise source and, in the rf SQUID, would prevent the dispersive mode of operation. In dc SQUID applications, the depth of the modulation of the critical current by the applied flux diminishes with increasing number of series junctions present in the SQUID loop, and the period of modulation may become erratic. Loops containing similar series junctions will always operate in the hysteretic regime.

In general, it is shown that the inclusion of series array of Josephson junctions into a superconducting interferometer loop produces a highly unstable system with many available states.

Published experimental data indicate that both rf and dc SQUID's using granular high- $T_c$  materials are frequently troubled by excessive  $1/f$  noise,<sup>3</sup> including telegraphlike noise,<sup>3,12</sup> and spurious modulations.<sup>16</sup> Telegraphlike noise occurs not only in SQUID's but also in thin-film samples of apparently single-connected geometry.<sup>11</sup> These data, while not directly confirming the existence of serial junctions in the investigated samples, are not at variance with it. The development of a dynamic theory based on the RSJ model and experiments on systems with known parameters are needed for a better understanding of the problems examined in this paper from the limited point of view of the static theory.

#### ACKNOWLEDGMENTS

Many long and stimulating discussions with J. Zagroźniński are gratefully acknowledged. The author wishes also to thank Roman Sobolewski for careful reading of the manuscript. This work was supported by the Polish Government under Grant No. RPBP 01.9.

<sup>1</sup>M. S. Colclough, C. E. Gough, M. Keene, C. M. Muirhead, N. Thomas, J. S. Abell, and S. Sutton, *Nature* **328**, 47 (1987); C. M. Pegrum, J. R. Buckley, and M. Odehna, *IEEE Trans. Magn.* **MAG-25**, 872 (1989).

<sup>2</sup>G. Jung and J. Konopka, *Europhys. Lett.* **10**, 183 (1989).

<sup>3</sup>Cf., R. H. Koch, C. P. Umbach, G. J. Clark, P. Chaudhari, and R. B. Laibowitz, *Appl. Phys. Lett.* **51**, 200 (1987); B. Hauser, B. Klopman, D. Blank, and H. Rogalla, *IEEE Trans. Magn.* **MAG-25**, 919 (1989).

<sup>4</sup>A. Barone and G. Paterno, *Physics and Applications of the Josephson Effect* (Wiley, New York, 1982).

<sup>5</sup>A. K. Jain, K. K. Likharev, J. E. Lukens, and J. E. Sauvageau, *Phys. Rep.* **109**, 311 (1984).

<sup>6</sup>J. Talvacchio, M. G. Forrester, and A. I. Braginski, in *Science and Technology of Thin-Film Superconductors*, edited by R. McConnel and S. A. Wolf (Plenum, New York, 1989).

<sup>7</sup>V. N. Belykh, N. F. Pedersen, and O. H. Soerensen, *Phys. Rev. B* **16**, 4853 (1977); **16**, 4860 (1977).

- <sup>8</sup>K. K. Likharev, *Introduction to the Dynamics of Josephson Junctions* (Nauka, Moscow, 1985).
- <sup>9</sup>T. J. Reiger, D. J. Scalapino, and J. E. Mercereau, *Phys. Rev. B* **6**, 1734 (1972).
- <sup>10</sup>W. J. Skocpol, M. R. Beasley, and M. Tinkham, *J. Low Temp. Phys.* **16**, 145 (1974).
- <sup>11</sup>P. Rosenthal, R. H. Hammond, M. R. Beasley, R. Leoni, Ph. Lerch, and J. Clarke, *IEEE Trans. Magn.* **MAG-25**, 973 (1989); R. H. Ono, J. A. Beal, M. W. Cromar, P. M. Maniewich, and R. E. Howard, *ibid.* **MAG-25**, 976 (1989).
- <sup>12</sup>M. Matsuda, A. Matachi, and S. Kuriki, *IEEE Trans. Magn.* **MAG-25**, 1301 (1989).
- <sup>13</sup>Won-Tien Tsang and T. Van Duzer, *J. Appl. Phys.* **46**, 4573 (1975).
- <sup>14</sup>R. L. Peterson and C. A. Hamilton, *J. Appl. Phys.* **50**, 8135 (1979).
- <sup>15</sup>J. Zagrodziński (private communication).
- <sup>16</sup>J. C. Gallop, A. J. Marsh, W. J. Radcliffe, and C. D. Langham, in *Proceedings of the European Conference on High-T<sub>c</sub> Thin Films and Single Crystals, Ustroń, 1989*, edited by W. Gorzkowski, M. Gutowski, A. Reich, and H. Szymczak, (World-Scientific, Singapore, 1990).